ISSN 0915-633X

NATIONAL INSTITUTE FOR FUSION SCIENCE

Complete Suppression of Pfirsch-Schlüter Current in a Toroidal $l=3$ Stellarator

Y. Sato, M. Yokoyama, M. Wakatani and V. D. Pusovitov

(Received - Sep. 21, 1999)

NIFS-612 Oct. 1999

RESEARCH REPORT
NIFS Series

NAGOYA, JAPAN

Complete Suppression of Pfirsch-Schlüter Current in a Toroidal $l = 3$ Stellarator

Yasuhiko Sato, Masayuki Yokoyama*, Masahiro Wakatani and Vladimir D. Pustovitov**

Graduate School of Energy Science
Kyoto University
Gokasho, Uji, Japan 611-0011
*National Institute for Fusion Science, Oroshi, Toki, Japan 509-5292
**Russian Research Center "Kurchatov Institute", Moscow 123182, Russian Federation

Abstract

Pfirsch-Schlüter (P-S) current is an inherent property of a finite pressure toroidal equilibrium of tokamak and stellarator. However, it was pointed out recently (V. D. Pustovitov, Nuclear Fusion **36** (1996) 583) that the P-S current would be suppressed completely if the external vertical field could be adjusted to satisfy the condition $\Omega = \langle\Omega\rangle$ in an $\ell = 3$ stellarator. Here $\Omega = \langle\tilde{B}^2\rangle/B_0^2 - 2\epsilon\cos\theta$, l is a pole number, $|\tilde{B}|$ the vacuum helical magnetic field, B_0 the toroidal field, ϵ the inverse aspect ratio, θ the poloidal angle and $\langle ...\rangle$ denotes the average over the toroidal angle. An example of such a stellarator equilibrium is presented in this paper. For this stellarator equilibrium, behavior of rotational transform and Boozer magnetic spectrum is clarified when the pressure is increased. Both formation of helical magnetic axis and reduction of toroidal curvature are important ingredients to reduce the P-S current. However, the collisionless particle confinement is not improved in this example.

Keywords

Pfirsch-Schlüter current, external vertical field, toroidal curvature, collisonless particle confinement

1. Introduction

Recently a potential freedom for designing a stellarator magnetic configuration is widely recognized, and new types of stellarator are constructed to investigate physics of stellarator plasmas. Large Helical Device (LHD) [1] started experiments at 1.5T in 1998. TJ-II [2] also showed initial experimental results in 1998. HSX [3] and Heliotron-J [4] experiments will start soon. The optimized stellarator W7-X [5] is under construction. In these ten years understanding of stellarator physics is significantly progressed for equilibrium, stability, transport and heating [6]. Although confinement properties are shown comparable to tokamak plasmas, the obtained highest beta, $\bar{\beta} \simeq 2.1\%$ in CHS [7], is fairly lower than $\bar{\beta} \simeq 30\%$ in START [8], where $\bar{\beta}$ is a volume average beta value.

The beta limit depends on both the equilibrium and stability properties. Here our concern is MHD equilibrium of stellarator.

It is known that the equilibrium beta limit, β_{eq}, is related to the Shafranov shift. One practical way to define β_{eq} is to take it equal to the β value when the Shafranov shift becomes a half of minor radius [6, 9, 10]. This estimation is useful when existence of flux surfaces is assumed in calculating stellarator equilibria.

The Shafranov shift is directly related to the Pfirsch-Schlüter (P-S) current which produces a vertical magnetic field to shift the equilibrium position. Since the Shafranov shift is roughly proportional to $\bar{\beta}/\beta_{eq}$, reduction of the Shafranov shift and corresponding increase in β_{eq} is favorable to obtain high beta equilibria. Recently Pustovitov presented methodology to suppress the P-S current completely in large aspect ratio conventional stellarators [11]. This approach is valid to explain the Heliotron E experimental results obtained by Besshou et al. [12, 13]. In conventional stellarators, the key ingredient to suppress the P-S current is the vertical field. It is noted that the MHD equilibrium without the Shafranov shift coincides with the zero P-S current equilibrium, since an additional vertical field due to the finite beta effect is not generated.

In this paper we show stellarator equilibria without the P-S current or the Shafranov shift. As Pustovitov pointed out [11, 14], stellarator equilibria with negligible P-S current have been presented in old papers [15, 16]. Since these interesting but scarce old results have been neither discussed nor developed theoretically, there is an evident lack of information on MHD equilibrium without the P-S current. Here we will discuss our new examples of MHD equilibrium without the Shafranov shift based on newly developed theoretical models. The important data are the magnetic spectra in the Boozer coordinates [17] for various beta values. The variation of rotational transform due to the finite beta effect is also examined.

It is interesting that in the Boozer coordinates our example $l = 3$ configuration has both the $l = 1$ and $l = 0$ (satellite of $l = 1$) components dominantly, and a relatively small component corresponding to the toroidal effect, where ℓ is a pole number. These results have similarity to the W7-AS and W7-X configurations [18, 19]. It is reminded that the W7-AS was firstly designed to reduce the P-S current compared to standard stellarators. In W7-X, the collisionless trapped particle confinement is not good at zero beta, but its confinement is improved when the beta value is increased. It is noted that the collisionless trapped particle confinement is not improved in W7-AS [19].

One difference between our example configuration and the W7-X configuration is related to the magnetic well. There is no magnetic well in our configuration. Probably we need a trade-off between the reduction of P-

S current (or Shafranov shift) and the formation of magnetic well.

In Section 2, the condition to eliminate the P-S current is shown. In Section 3, a coil configuration for the $\ell = 3$ stellarator is introduced for studying the zero P-S current equilibrium. In Section 4, it is demonstrated that the Shafranov shift due to the P-S current is completely suppressed in finite beta stellarator plasmas. The properties of these MHD equilibria are also shown. Finally, collisionless particle confinement is examined. In Section 5, concluding remarks are given.

2. Condition for Zero Pfirsch-Schlüter Current MHD Equilibrium

Let us recall some theoretical arguments on P-S current suppression in conventional stellarators [11, 14]. The general expression for the P-S current in conventional stellarators with planar circular axis and helical magnetic field can be written as

$$J_\zeta = 2\pi R P'(\psi)(\Omega - \langle\Omega\rangle) \ . \qquad (1)$$

Here, R is a major radius, P is a plasma pressure, ψ is a poloidal flux, Ω is a quantity characterizing the inhomogeneity of the magnetic field,

$$\Omega = \frac{\langle \hat{\boldsymbol{B}} \rangle^2}{B_0^2} - \frac{2\rho}{R}\cos\theta \ , \qquad (2)$$

where $\hat{\boldsymbol{B}}$ is the vacuum helical magnetic field. B_0 is the toroidal field at the geometrical axis. Here $(\rho,\ \theta,\ \zeta)$ are quasi-cylindrical coordinates. In Eq. (1) the prime denotes the derivative with respect to ψ. Also $\langle ... \rangle$ stands for averaging over the toroidal coordinate ζ. It is noted that expression (1) is valid for any shape of magnetic surfaces. From Eq. (1) for the P-S current, its right hand side becomes identically zero if $\Omega = \langle\Omega\rangle$. This is equivalent to the condition

$$\Omega = \Omega(\psi) \ . \qquad (3)$$

In conventional stellarators the ψ dependent magnetic field is given by

$$\boldsymbol{B}_p = \frac{1}{2\pi}\boldsymbol{\nabla}(\psi - \psi_V) \times \nabla\zeta \ , \qquad (4)$$

where $\boldsymbol{B}_p$ is the axisymmetric component of the poloidal magnetic field, and ψ_V is the poloidal flux of the helical magnetic field $\hat{\boldsymbol{B}}$ given by

$$\psi_V = \frac{2\pi r^3}{R B_0}\langle \hat{B}_z \int \hat{B}_r d\zeta \rangle \ . \qquad (5)$$

Here $(r,\ z)$ are components of cylindrical coordinates, and r corresponds to the major radius. In all expressions here, the function ψ does not depend on ζ. This allows the condition (3) to be written as

$$\nabla\psi \times \nabla\zeta \cdot \nabla\Omega = 0 \ . \qquad (6)$$

Finally, using Eq. (4), we arrive to an equivalent differential formulation of the condition,

$$\left(\boldsymbol{B}_p + \frac{\boldsymbol{\nabla}\psi_V \times \boldsymbol{\nabla}\zeta}{2\pi}\right) \cdot \boldsymbol{\nabla}\Omega = 0 \ . \qquad (7)$$

For analyzing this condition, it is sufficient to substitute the vacuum field for $\boldsymbol{B}_p$ into Eq. (7) because there is no additional poloidal

magnetic field in the absence of a P-S current. Another attractive feature of Eq. (7), as compared with the initial condition (3), is that it is written in an invariant form, which facilitates its use in analytical or numerical calculations.

According to Pustovitov [11], Eq. (7) can be written for stellarators with $\psi_V = \psi_V(\rho)$ as

$$2B_0\rho\mu_h + B_\perp \frac{m(\rho^4\mu_h)'}{\ell\rho^2} = 0\ , \qquad (8)$$

where the prime denotes the derivative with respect to ρ, and m is a pitch number in the toroidal direction. This equation is given by using the relation between $\psi_V(\rho)$ and the vacuum rotational transform $\mu_h(\rho)$.

$$\psi_V = -2\pi B_0 \int \rho\mu_h(\rho)d\rho \qquad (9)$$

and

$$\frac{\boldsymbol{\nabla}\psi_V \times \boldsymbol{\nabla}\zeta}{2\pi} \cdot \boldsymbol{\nabla}\Omega = 2B_0\mu_h \frac{\rho}{R^2}\sin\theta\ , \quad (10)$$

where the first term Ω_0 in Eq. (2) is also assumed to be a function of an average minor radius ρ. In Eq. (8) $B_\perp$ denotes an additional vertical field in the vertical or z-direction on the equatorial plane. whose contribution into Eq. (7) is given as

$$B_\perp \boldsymbol{e}_z\cdot\boldsymbol{\nabla}\Omega = B_\perp \boldsymbol{e}_z\cdot\boldsymbol{\nabla}\Omega_0 = B_\perp \frac{m(\rho^4\mu_h)'}{\ell R^2\rho^2}\sin\theta\ . \qquad (11)$$

Equation (8) has a solution expressed as

$$\mu_h = \mu_{h0}\rho^{-(C+4)}, \qquad (12)$$

where μ_{h0} is a constant and ρ the dimensionless radius and $C = 2lB_0/(mB_\perp)$. Equating $-(C+4) = 2(l-2)$ based on the analytical expression of μ_h as $\mu_h = \mu_{h0}\rho^{2(l-2)}$ [20] leads to the relation,

$$\frac{B_\perp}{B_0} = -\frac{1}{m}. \qquad (13)$$

This expression is valid for shearless (or in the region close to the magnetic axis in) $l = 2$ stellarators and for stellarators with $l \gtrsim 3$.

3. Coil Configuration of $\ell = 3$ Stellarator for Suppressing Shafranov Shift

In Ref. [16] the MHD equilibrium was solved numerically with a prescribed pressure profile for an $\ell = 3$ large aspect ratio stellarator with $R/a = 16$, where a is a radius of plasma column. It was shown there that at $\bar{\beta} = 2.5\%$ the magnetic configuration was geometrically the same as the vacuum configuration if a vertical field with an amplitude of $|B_\perp|/B_0 = 0.05$ was applied to shift the magnetic axis inward. Since $m = 20$ for this example. Eq. (13) gives $B_\perp$ consistent with the numerical result. This $\ell = 3$ stellarator seems more realistic compared to the other mentioned numerical example of interest for $l = 2$ stellarator with an extremely large aspect ratio $R/a = 100$ [17], where the pitch number was also too large. $m = 100$. Here we pick up an $l = 3$ stellarator similar to that given in Ref. [16]. The coil parameters are shown in Table 1. Overview of the coil system described in Table 1 is demonstrated in Fig.1. In Fig.1 all coils have finite cross-sections: however. for the numerical calcula-

tion of vacuum flux surfaces shown in Fig.2 (a), filamentary coils are employed for simplicity. Three cross-sections of flux surfaces at $\zeta = 0$, $\zeta = 2\pi/4m$ and $\zeta = 2\pi/2m$ are shown here. It is noted that the average minor radius is 72cm, which corresponds to an aspect ratio of 5.6 (compare with 16 in Ref. [16]), and the magnetic axis exists at 3.42m which is already shifted inward compared to the geometrical major radius. Figures 2 (b) and 2 (c) show corresponding rotational transform and magnetic well (hill) depth given by $(V''(0)-V''(v))/V''(0)$, where v is the toroidal magnetic flux and V is the plasma volume within a $v = const$ surface. Unfortunately, the magnetic configuration shown in Fig.1 and Fig.2 may not be suitable for high beta plasma confinement, since the rotational transform in the central region is fairly small and the whole plasma region belongs to the magnetic hill. However, from the point of view of collisionless trapped particle confinement, this configuration has a good property that the minimum of $|\boldsymbol{B}|$ in the ripple field along the magnetic field line does not depend on the toroidal angle, which is favorable for the collisionless particle confinement [21].

pole number (ℓ)	3
pitch number (m)	18
major radius of helical coil	4.0 (m)
minor radius of helical coil	1.27 (m)
major radius of vertical coil	6.36 (m)
height of vertical coil from horizontal plane	± 2.18 (m)
major radius of toroidal coil	4.0 (m)
minor radius of toroidal coil	2.18 (m)
helical coil current	$\pm 5.0 \times 10^5$ (A)
vertical coil current	4.0×10^3 (A)
toroidal coil current	3.0×10^5 (A)

Table 1 Coil parameters of $\ell = 3$ Stellarator

4. Properties of Zero Pfirsch-Schlüter Current MHD Equilibrium

Finite beta MHD equilibria of the $\ell = 3$ stellarator given in Table 1 are calculated with the VMEC [22] by changing the vertical magnetic field. Here the pressure profile is assumed as

$$P = P_0(1 - s)^2 , \qquad (14)$$

where s is the normalized toroidal magnetic flux. The vacuum outermost flux surface is fixed during the MHD equilibrium calculations. Here we will pick up three cases of the vertical field for adjusting the magnetic axis position; case (I) $R_{axis} = 3.42$m with $B_\perp/B_0 = 2.46\times10^{-3}$, case (II) $R_{axis} = 3.19$m with $B_\perp/B_0 = 2.45 \times 10^{-2}$ and case (III) $R_{axis} = 3.17$m with $B_\perp/B_0 = 3.20 \times 10^{-2}$, where R_{axis} denotes the radius of magnetic axis. It is noted that case (I) corresponds to the configuration shown in Fig.2 (a).

The Shafranov shift for these three cases is shown in Fig.3. The origin of the Shafranov shift is the P-S current which generates

the vertical field. It is seen that the Shafranov shift is almost completely suppressed for the case (II). Also the Shafranov shift is over-compensated by the vertical field for the case (III): the shift is inward in this case. As mentioned in Sec.3, the case (I) has a significantly large Shafranov shift even for low beta equilibria due to the fairly small rotational transform. The almost complete suppression of Shafranov shift in the case (II) is also valid for the different pressure profile, which is understood from Eq. (13) without the pressure profile dependence.

The vacuum flux surfaces of the case (II) are shown in Fig.4 (a). The shape of the outermost flux surface is quite different from that in Fig.2 (a) (case (I)). The rotational transform and the magnetic well (or hill) are shown in Fig.4 (b) and Fig.4 (c), respectively, for $\bar{\beta} = 0\%$. It is noted that the aspect ratio is about 13 for the case (II). This example demonstrates that the stellarator equilibrium without the P-S current is realistic. It is noted that the W7-AS stellarator was designed to reduce the P-S current compared to a standard stellarator.

It is interesting to check whether the reduction of P-S current correlates with the improvement of collisionless trapped particle confinement or not. For the case of W7-X, the particle confinement has a tendency to be improved by reducing the P-S current; however, it is not significant in W7-AS. The largest five magnetic spectra (except $B_{0,0}$) in the Boozer coordinates for the case (II) are shown in Fig.5 (a) and Fig.5 (b) for $\bar{\beta} = 0\%$ and 1.46%, respectively. Here it is noted that the line for $B_{0,0}$ denotes the difference, $B_{0,0}(r/a) - B_{0,0}(0)$, and all other components are normalized by $B_{0,0}(0)$. The toroidal mode number is normalized by the toroidal pitch number, m. It is interesting that the magnetic spectra do not depend on the plasma pressure. This is also an indication that the P-S current which change a magnetic configuration with a finite pressure is negligibly small. It is noted that the bumpy component $B_{0,1}$ and the $\ell = 1$ helical component $B_{1,1}$ are large. As a reference, vacuum magnetic spectra for the case (I) are shown in Fig.6. It is noted that $B_{3,1}$ and $B_{1,0}$ components are large at the edge region; however, the contribution from $B_{0,0}$ and $B_{2,0}$ components increases at inner region. Figure 7 shows the variation of rotational transform due to the finite beta effect for the case (II). The central value of rotational transform increases also in this case.

In order to examine the efficiency of collisionless particle confinement, particle orbits are followed for the three cases (I), (II) and (III). The case (I) shows the best confinement as shown in Fig.8. Although the toroidal effect corresponding to the magnetic component $B_{1,0}$ in Fig.5 (a) is reduced, there exists still several fairly large helical com-

ponents which may degrade the collisionless particle confinement. It is interesting that the local minimum values of B is almost independent of the poloidal angle for the case (I), although the cases (II) and (III) do not show such a tendency. Since these is no alignment of the local minimum of B in the case (II), improvement of trapped particle confinement is weak, although the P-S current has been suppressed.

5. Concluding Remarks

The stellarator configuration without the P-S current or Shafranov shift has been demonstrated successfully. It is also shown that the magnetic spectra do not depend on the plasma pressure. However, from the point of view of collisionless trapped particle confinement, the complete suppression of P-S current is not always favorable. Thus it is important to design a stellarator by optimizing three points of view: reduction of P-S current, collisionless trapped particle confinement and formation of magnetic well with subtle trade-offs.

References

[1] IIYOSHI, A., et al., Proc. IAEA Conf. on Fusion Energy (Yokohama, 1998) IAEA-CN-69/OV1/4.

[2] ALEJALDRE, C., Fusion Technol. **17** (1990) 131.

[3] ANDERSON, D. T., et al., HSX-A Helically Symmetric Toroidal Experiment (edited by Torsatron/Stellarator Laboratory, Univ. of Wisconsin, 1998)

[4] WAKATANI, M., et al., Proc. IAEA Conf. on Fusion Energy (Yokohama, 1998) IAEA-F1-CN-69/ICP/08(R).

[5] GRIEGER, G., et al., Proc. IAEA Conf. on Plasma Phys. Controlled Nuclear Fusion Research (Nice, 1988) (IAEA, Vienna, 1989) vol.2, p.369.

[6] WAKATANI, M., *Stellarator and Heliotron Devices*, Oxford University Press, 1998.

[7] OKAMURA, S., et al., Nucl. Fusion **35** (1995) 283.

[8] GATES, D. A., et al., Phys. Plasmas **5** (1998) 1775.

[9] CARRERAS, B. A., et al., Nucl. Fusion **28** (1988) 1613.

[10] PUSTOVITOV, V. D., J. Plasma Fusion Res. (formerly Kakuyugo Kenkyu) **70** (1994) 943.

[11] PUSTOVITOV, V. D., Nucl. Fusion **36** (1996) 583.

[12] BESSHOU, S., et al., Nucl. Fusion **35** (1995) 173.

[13] BESSHOU, S., PUSTOVITOV, V. D., et al., Phys. Plasmas **5** (1998) 481.

[14] PUSTOVITOV, V. D., Nucl. Fusion **36** (1996) 1281.

[15] GREENE, J. M., JOHNSON, J. L., Phys. Fluids **4** (1961) 875.

[16] GREENE, J. M., et al., Plasma Phys. **8** (1966) 145.

[17] BOOZER, A. H., Phys. Fluids **23** (1980) 904.

[18] WELLER, A., et al., Plasma Phys. Controlled Fusion **33** (1991) 1559.

[19] GRIEGER, G., et al., Phys. Fluids **B 4** (1992) 2081.

[20] MOROZOV, A. I., SOLOV'EV, L. S., *Reviews of Plasma Physics*, New York: Consultants Bureau, (1966) Vol.2, p.1.

[21] MYNICK, H. E., Phys. Fluids **26** (1983) 2609.

[22] HIRSHMAN, S. P., et al., Comput. Phys. Commun. **43** (1986) 143.

Figure Captions

Fig.1 Coil configuration of $\ell = 3$ stellarator for studying reduction of P-S current.

Fig.2 (a) Vacuum flux surfaces, (b) vacuum rotational transform and (c) vacuum magnetic well (hill) defined by $(V'(0) - V'(\psi))/V'(0)$ for the $\ell = 3$ stellarator corresponding to parameters shown in Table 1.

Fig.3 Shafranov shift of $\ell = 3$ stellarator as a function of average beta for different vertical fields, cases (I), (II) and (III).

Fig.4 (a) Vacuum flux surfaces, (b) vacuum rotational transform and (c) vacuum magnetic well (hill) for the case (II).

Fig.5 Magnetic spectra for the case (II) at (a) $\bar{\beta} = 0\%$, and (b) $\bar{\beta} = 1.46\%$.

Fig.6 Magnetic spectra for the case (I) at $\bar{\beta} = 0\%$.

Fig.7 Variation of rotational transform profile for the case (II) due to the finite beta effect.

Fig.8 Collisionless particle losses in the three vertical field cases (I), (II) and (III) as a function of the time of flight. Particles (protons with $\rho_i/a = 4.5 \times 10^{-3}$) are started at $r/a = 0.5$ and 0.75, which are uniformly distributed in both the real space and the velocity space. Here ρ_i is an ion Larmor radius, a is a plasma minor radius and r denotes a radius defined by the toroidal flux function.

Fig.9 Magnitude of $|\boldsymbol{B}|$ along the magnetic field line on the flux surface at $r/a = 0.5$ for three vertical field cases (I), (II) and (III).

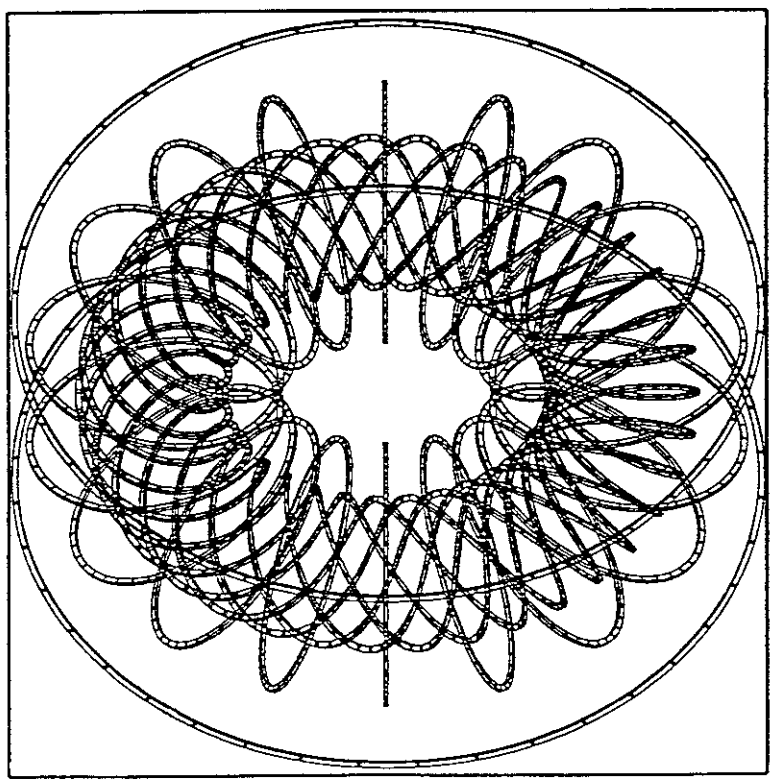

Fig. 1

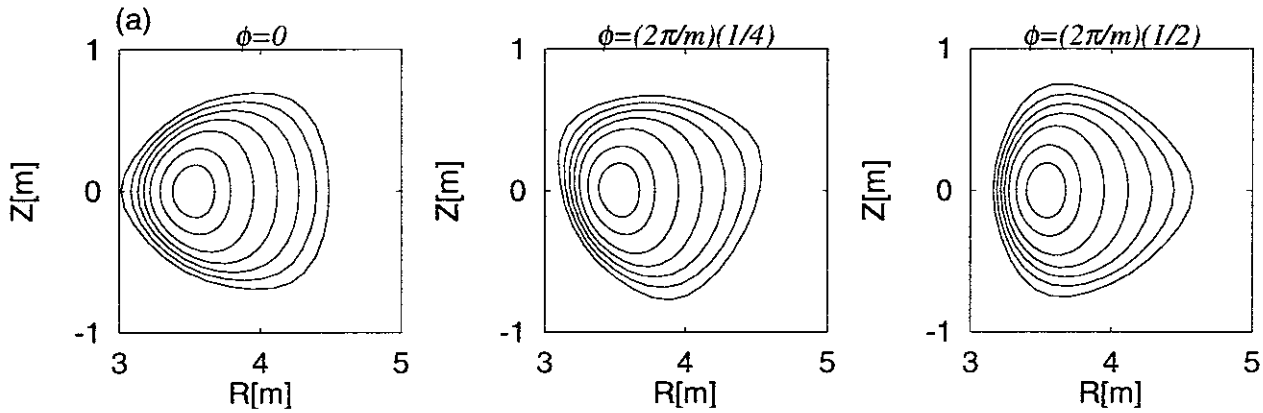
(a)
φ=0
φ=(2π/m)(1/4)
φ=(2π/m)(1/2)
Z[m]
R[m]
1
0
-1
3
4
5

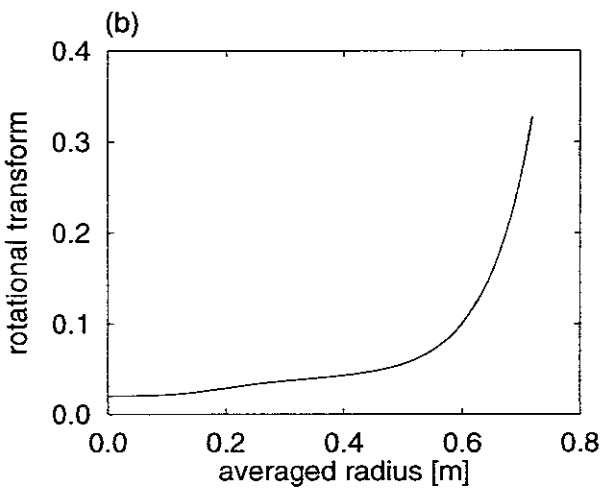
(b)
rotational transform
averaged radius [m]
0.0
0.1
0.2
0.3
0.4
0.6
0.8

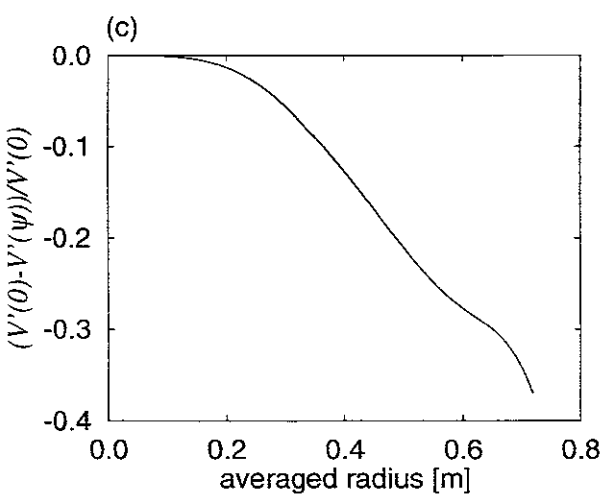
(c)
(V'(0)-V'(ψ))/V'(0)
averaged radius [m]
0.0
-0.1
-0.2
-0.3
-0.4
0.6
0.8

Fig. 2

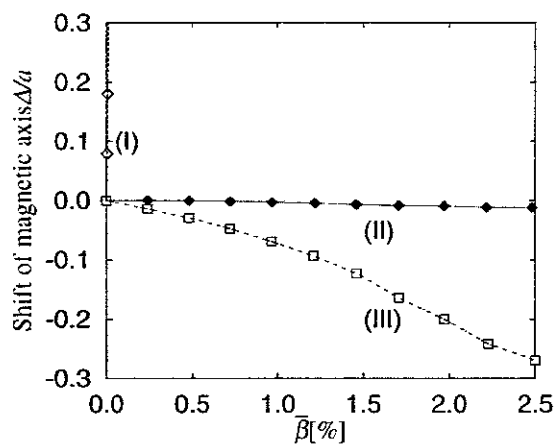
Shift of magnetic axis Δ/a
β̄[%]
(I)
(II)
(III)
0.3
0.2
0.1
0.0
-0.1
-0.2
-0.3
0.5
1.0
1.5
2.0
2.5

Fig. 3

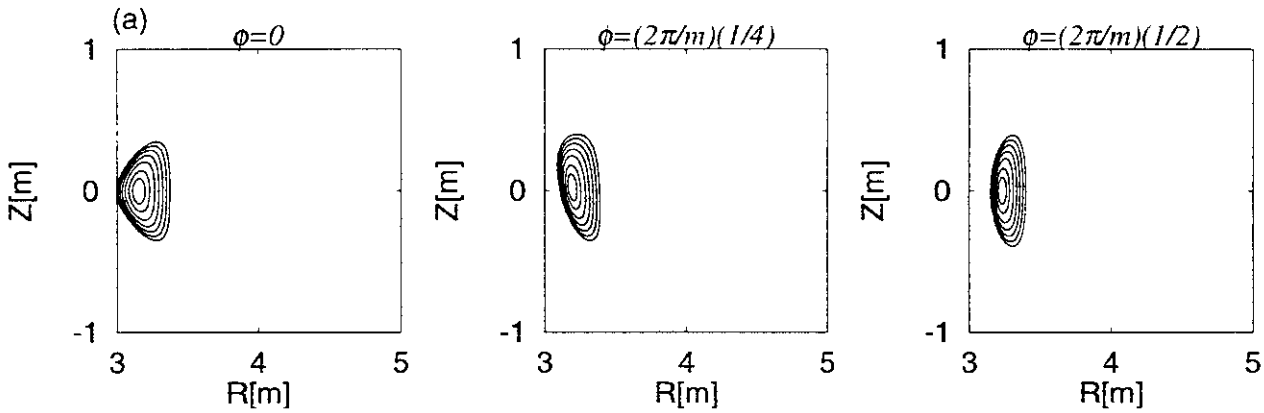
(a)
φ=0
φ=(2π/m)(1/4)
φ=(2π/m)(1/2)
Z[m]
R[m]
1
0
-1
3
4
5

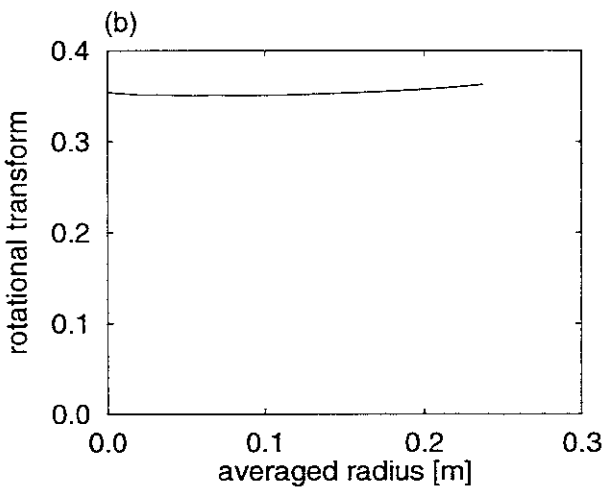
(b)
rotational transform
averaged radius [m]
0.0
0.1
0.2
0.3
0.4

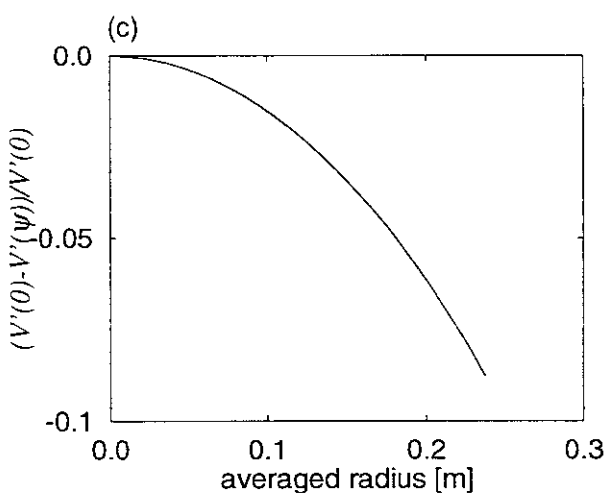
(c)
(V'(0)-V'(ψ))/V'(0)
averaged radius [m]
0.0
-0.05
-0.1
0.1
0.2
0.3

Fig. 4

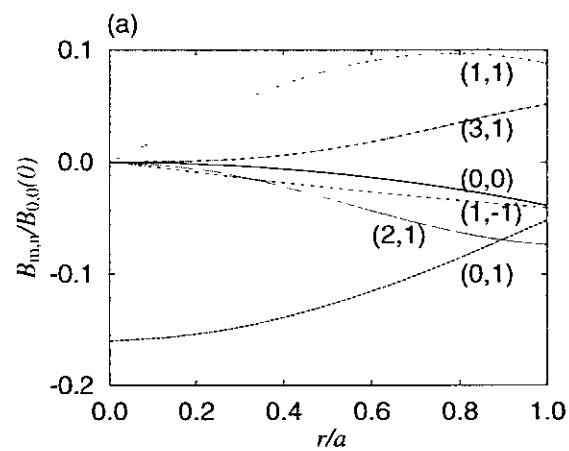
(a)
$B_{m,n}/B_{0,0}(0)$
r/a
(1,1)
(3,1)
(0,0)
(1,-1)
(2,1)
(0,1)
0.1
0.0
-0.1
-0.2
0.2
0.4
0.6
0.8
1.0

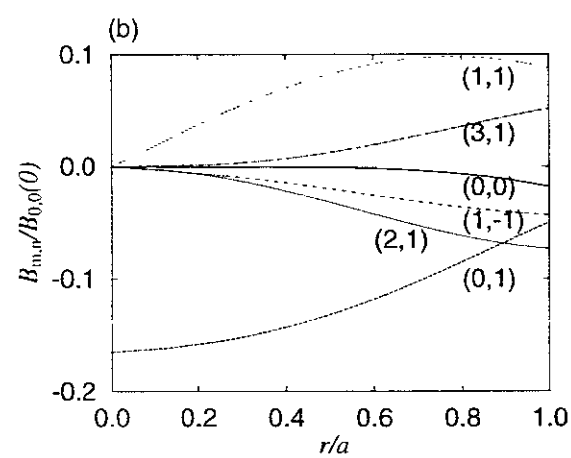
(b)
$B_{m,n}/B_{0,0}(0)$
r/a
(1,1)
(3,1)
(0,0)
(1,-1)
(2,1)
(0,1)
0.1
0.0
-0.1
-0.2
0.2
0.4
0.6
0.8
1.0

Fig. 5

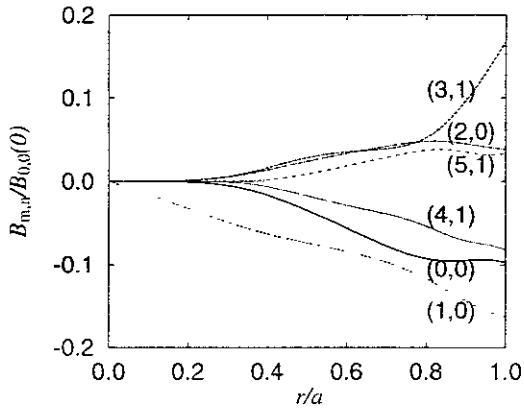

Fig. 6

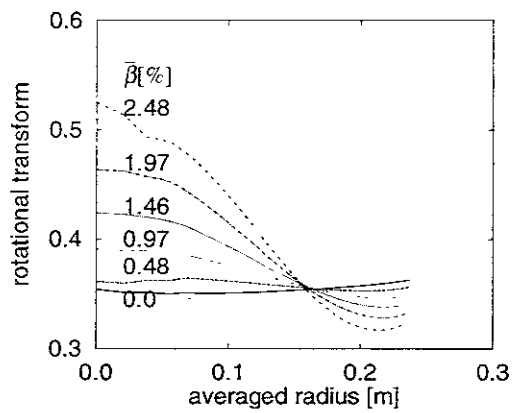

Fig. 7

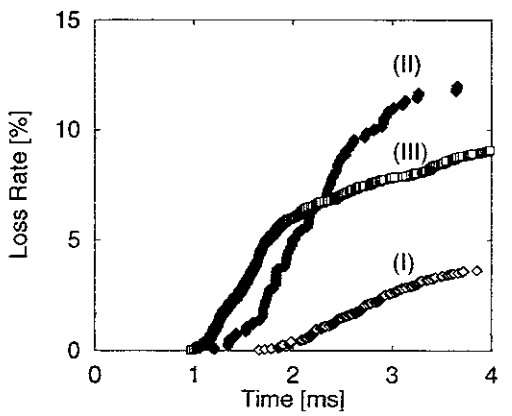

Fig. 8

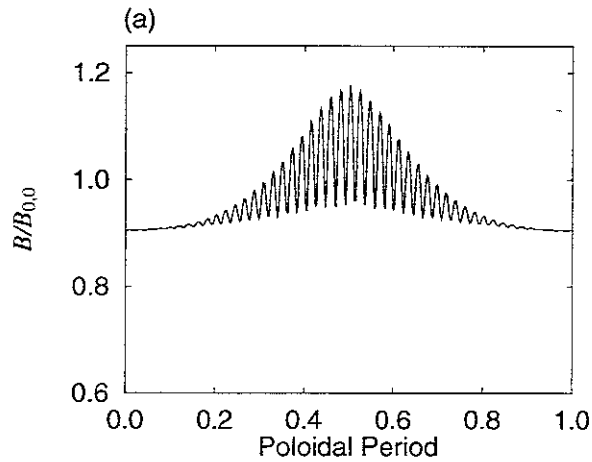

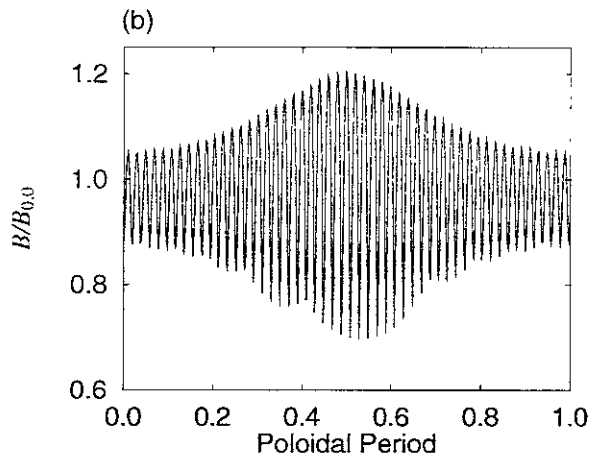

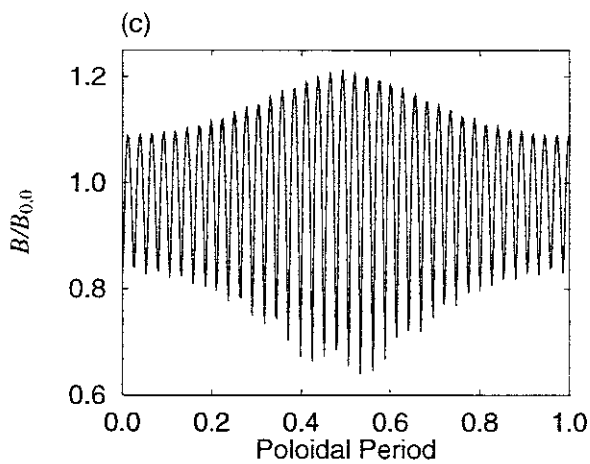

Fig. 9

Recent Issues of NIFS Series

NIFS-549 M.M Skoric, T Sato, A M Maluckov and M S. Jovanovic,
On Kinetic Complexity in a Three-Wave Interaction, June 1998

NIFS-550 S Goto and S Kida,
Passive Saclar Spectrum in Isotropic Turbulence: Prediction by the Lagrangian Direct-interaction Approximation; June 1998

NIFS-551 T Kuroda, H. Sugama, R. Kanno, M Okamoto and W Horton,
Initial Value Problem of the Toroidal Ion Temperature Gradient Mode ; June 1998

NIFS-552 T Mutoh, R. Kumazawa, T Seki, F. Simpo, G. Nomura, T Ido and T Watari,
Steady State Tests of High Voltage Ceramic Feedthoughs and Co-Axial Transmission Line of ICRF Heating System for the Large Helical Device , June 1998

NIFS-553 N. Noda, K. Tsuzuki, A Sagara, N. Inoue, T Muroga,
oronaization in Future Devices -Protecting Layer against Tritium and Energetic Neutrals-: July 1998

NIFS-554 S Murakami and H Saleem,
Electromagnetic Effects on Rippling Instability and Tokamak Edge Fluctuations, July 1998

NIFS-555 H. Nakamura , K. Ikeda and S Yamaguchi,
Physical Model of Nernst Element, Aug. 1998

NIFS-556 H Okumura, S Yamaguchi, H Nakamura, K. Ikeda and K Sawada,
Numerical Computation of Thermoelectric and Thermomagnetic Effects; Aug 1998

NIFS-557 Y Takein, M. Osakabe, K. Tsumori, Y Oka, O. Kaneko, E Asano, T Kawamoto, R. Akiyama and M Tanaka,
Development of a High-Current Hydrogen-Negative Ion Source for LHD-NBI System, Aug 1998

NIFS-558 M. Tanaka, A Yu Grosberg and T. Tanaka,
Molecular Dynamics of Structure Organization of Polyampholytes, Sep 1998

NIFS-559 R. Horiuchi, K Nishimura and T. Watanabe,
Kinetic Stabilization of Tilt Disruption in Field-Reversed Configurations; Sep 1998
(IAEA-CN-69/THP1/11)

NIFS-560 S. Sudo, K. Kholopenkov, K Matsuoka, S. Okamura, C. Takahashi, R Akiyama, A. Fujisawa, K. Ida, H Idei, H. Iguchi, M. Isobe, S Kado, K. Kondo, S Kubo, H. Kuramoto, T. Minami, S Morita, S Nishimura, M. Osakabe, M. Sasao, B Peterson, K. Tanaka, K Toi and Y. Yoshimura,
Particle Transport Study with Tracer-Encapsulated Solid Pellet Injection; Oct 1998
(IAEA-CN-69/EXP1/18)

NIFS-561 A. Fujisawa, H. Iguchi, S. Lee, K. Tanaka, T. Minami, Y Yoshimura, M Osakabe, K Matsuoka, S Okamura, H. Idei, S. Kubo, S Ohdachi, S. Morita, R. Akiyama, K. Toi, H Sanuki, K Itoh, K. Ida, A Shimizu, S Takagi, C. Takahashi, M. Kojima, S Hidekuma, S. Nishimura, M Isobe, A Ejiri, N. Inoue, R. Sakamoto, Y. Hamada and M Fujiwara,
Dynamic Behavior Associated with Electric Field Transitions in CHS Heliotron/Torsatron, Oct 1998
(IAEA-CN-69/EX5/1)

NIFS-562 S. Yoshikawa,
Next Generation Toroidal Devices; Oct 1998

NIFS-563 Y. Todo and T Sato,
Kinetic-Magnetohydrodynamic Simulation Study of Fast Ions and Toroidal Alfvén Eigenmodes; Oct. 1998
(IAEA-CN-69/THP2/22)

NIFS-564 T. Watari, T. Shimozuma, Y. Takein, R Kumazawa, T. Mutoh, M. Sato, O. Kaneko, K Ohkubo, S. Kubo, H. Idei, Y Oka, M. Osakabe, T. Seki, K. Tsumori, Y. Yoshimura, R. Akiyama, T Kawamoto, S. Kobayashi, F. Shimpo, Y Takita, E Asano, S Itoh, G. Nomura, T. Ido, M. Hamabe, M. Fujiwara, A Iiyoshi, S. Morimoto, T Bigelow and Y.P Zhao,
Steady State Heating Technology Development for LHD, Oct. 1998
(IAEA-CN-69/FTP/21)

NIFS-565 A. Sagara, K Y. Watanabe, K. Yamazaki, O. Motojima, M. Fujiwara, O. Mitarai, S. Imagawa, H. Yamanishi, H Chikaraishi, A. Kohyama, H. Matsui, T. Muroga, T. Noda, N. Ohyabu, T. Satow, A.A Shishkin, S Tanaka, T. Terai and T Uda,
LHD-Type Compact Helical Reactors; Oct 1998

(IAEA-CN-69/FTP/03(R)

NIFS-566 N. Nakajima, J. Chen, K. Ichiguchi and M. Okamoto,
Global Mode Analysis of Ideal MHD Modes in L=2 Heliotron/Torsatron Systems; Oct 1998
(IAEA-CN-69/THP1/08)

NIFS-567 K. Ida, M. Osakabe, K. Tanaka, T. Minami, S. Nishimura, S. Okamura, A. Fujisawa, Y. Yoshimura, S. Kubo, R. Akiyama, D.S.Darrow, H. Idei, H. Iguchi, M. Isobe, S. Kado, T. Kondo, S. Lee, K. Matsuoka, S. Morita, I. Nomura, S. Ohdachi, M. Sasao, A. Shimizu, K. Tumon, S. Takayama, M. Takechi, S. Takagi, C. Takahashi, K. Toi and T. Watari,
Transition from L Mode to High Ion Temperature Mode in CHS Heliotron/Torsatron Plasmas; Oct. 1998
(IAEA-CN-69/EX2/2)

NIFS-568 S. Okamura, K. Matsuoka, R. Akiyama, D.S. Darrow, A. Ejiri, A. Fujisawa, M. Fujiwara, M. Goto, K. Ida H. Idei, H. Iguchi, N. Inoue, M. Isobe, K. Itoh, S. Kado, K. Khlopenkov, T. Kondo, S. Kubo, A. Lazaros, S. Lee, G. Matsunaga, T. Minami, S. Morita, S. Murakami, N. Nakajima, N. Nikai, S. Nishimura, I Nomura, S. Ohdachi, K. Ohkuni, M. Osakabe, R. Pavlichenko, B. Peterson, R. Sakamoto, H. Sanuki, M. Sasao, A. Shimizu, Y. Shirai, S. Sudo, S. Takagi, C Takahashi, S. Takayama, M. Takechi, K. Tanaka, K. Toi, K Yamazaki, Y Yoshimura and T Watari,
Confinement Physics Study in a Small Low-Aspect-Ratio Helical Device CHS; Oct. 1998
(IAEA-CN-69/OV4/5)

NIFS-569 M.M. Skoric, T. Sato, A. Maluckov, M.S. Jovanovic,
Micro- and Macro-scale Self-organization in a Dissipative Plasma; Oct. 1998

NIFS-570 T. Hayashi, N. Mizuguchi, T-H. Watanabe, T. Sato and the Complexity Simulation Group,
Nonlinear Simulations of Internal Reconnection Event in Spherical Tokamak; Oct. 1998
(IAEA-CN-69/TH3/3)

NIFS-571 A. Iiyoshi, A. Komori, A. Ejiri, M. Emoto, H. Funaba, M Goto, K. Ida, H. Idei, S. Inagaki, S. Kado, O. Kaneko, K. Kawahata, S. Kubo, R. Kumazawa, S. Masuzaki, T. Minami, J. Miyazawa, T. Morisaki, S. Morita, S. Murakami, S. Muto, T. Muto, Y. Nagayama, Y. Nakamura, H. Nakanishi, K. Narihara, K. Nishimura, N Noda, T Kobuchi, S. Ohdachi, N. Ohyabu, Y Oka, M. Osakabe, T. Ozaki, B.J. Peterson, A. Sagara, S. Sakakibara, R Sakamoto, H. Sasao, M Sasao, K Sato, M. Sato, T Seki, T. Shimozuma, M. Shoji, H. Suzuki, Y Takeiri, K. Tanaka, K. Toi, T. Tokuzawa, K. Tsumori, I. Yamada, H. Yamada, S. Yamaguchi, M. Yokoyama, K.Y.Watanabe, T. Watari, R. Akiyama, H Chikaraishi, K. Haba, S. Hamaguchi, S. Iima, S. Imagawa, N. Inoue, K. Iwamoto, S. Kitagawa, Y. Kubota, J. Kodaira, R. Maekawa, T. Mito. T. Nagasaka, A. Nishimura, Y. Takita, C. Takahashi, K. Takahata, K. Yamauchi, H. Tamura, T Tsuzuki, S. Yamada, N. Yanagi, H. Yonezu, Y. Hamada, K. Matsuoka, K. Murai, K. Ohkubo, I. Ohtake, M. Okamoto, S. Sato, T. Satow, S. Sudo, S. Tanahashi, K. Yamazaki, M. Fujiwara and O. Motojima,
An Overview of the Large Helical Device Project; Oct. 1998
(IAEA-CN-69/OV1/4)

NIFS-572 M. Fujiwara, H. Yamada, A. Ejiri, M. Emoto, H. Funaba, M. Goto, K. Ida, H. Idei, S. Inagaki, S. Kado, O. Kaneko, K. Kawahata, A. Komori, S. Kubo, R. Kumazawa, S. Masuzaki, T. Minami, J. Miyazawa, T. Morisaki, S. Morita, S. Murakami, S. Muto, T. Muto, Y. Nagayama, Y. Nakamura, H. Nakanishi, K. Narihara, K. Nishimura, N. Noda, T. Kobuchi, S. Ohdachi, N. Ohyabu, Y. Oka, M. Osakabe, T. Ozaki, B. J. Peterson, A. Sagara, S. Sakakibara, R. Sakamoto, H. Sasao, M. Sasao, K. Sato, M. Sato, T. Seki, T. Shimozuma, M. Shoji, H. Sazuki, Y. Takeiri, K. Tanaka, K. Toi, T. Tokuzawa, K. Tsumori, I. Yamada, S. Yamaguchi, M. Yokoyama, K.Y. Watanabe, T. Watari, R. Akiyama, H. Chikaraishi, K. Haba, S. Hamaguchi, M. Iima, S. Imagawa, N. Inoue, K. Iwamoto, S. Kitagawa, Y. Kubota, J. Kodaira, R. Maekawa, T. Mito, T. Nagasaka, A. Nishimura, Y. Takita, C. Takahashi, K. Takahata, K. Yamauchi, H. Tamura, T. Tsuzuki, S. Yamada, N. Yanagi, H. Yonezu, Y. Hamada, K. Matsuoka, K. Murai, K. Ohkubo, I. Ohtake, M. Okamoto, S. Sato, T. Satow, S. Sudo, S. Tanahashi, K. Yamazaki, O. Motojima and A. Iiyoshi,
Plasma Confinement Studies in LHD; Oct. 1998
(IAEA-CN-69/EX2/3)

NIFS-573 O. Motojima, K. Akaishi, H. Chikaraishi, H. Funaba, S. Hamaguchi, S. Imagawa, S. Inagaki, N. Inoue, A. Iwamoto, S. Kitagawa, A. Komori, Y. Kubota, R. Maekawa, S. Masuzaki, T. Mito, J Miyazawa, T. Morisaki, T. Muroga, T. Nagasaka, Y. Nakmura, A. Nishimura, K. Nishimura, N. Noda, N Ohyabu, S. Sagara, S. Sakakibara, R. Sakamoto, S. Satoh, T. Satow, M. Shoji, H. Suzuki, K. Takahata, H. Tamura, K. Watanabe, H. Yamada, S Yamada, S. Yamaguchi, K. Yamazaki, N. Yanagi, T. Baba, H. Hayashi, M. Iima, T. Inoue, S. Kato, T Kato, T. Kondo, S. Moriuchi, H Ogawa, I Ohtake, K. Ooba, H. Sekiguchi, N. Suzuki, S. Takami, Y. Taniguchi, T. Tsuzuki, N. Yamamoto, K. Yasui, H. Yonezu, M. Fujiwara and A. Iiyoshi,
Progress Summary of LHD Engineering Design and Construction; Oct. 1998
(IAEA-CN-69/FT2/1)

NIFS-574 K. Toi, M. Takechi, S. Takagi, G. Matsunaga, M. Isobe, T Kondo, M Sasao, D.S. Darrow, K. Ohkuni, S. Ohdachi, R. Akiyama A. Fujisawa, M. Gotoh, H. Idei, K. Ida, H. Iguchi, S. Kado, M. Kojima, S. Kubo, S. Lee, K. Matsuoka, T. Minami, S. Morita, N. Nikai, S. Nishimura, S. Okamura, M Osakabe, A. Shimizu, Y. Shirai, C. Takahashi, K. Tanaka, T. Watari and Y. Yoshimura,
Global MHD Modes Excited by Energetic Ions in Heliotron/Torsatron Plasmas; Oct. 1998
(IAEA-CN-69/EXP1/19)

NIFS-575 Y. Hamada, A. Nishizawa, Y. Kawasumi, A. Fujisawa, M. Kojima, K. Narihara, K. Ida, A. Ejiri, S. Ohdachi, K. Kawahata, K. Toi, K. Sato, T. Seki, H. Iguchi, K. Adachi, S. Hidekuma, S.Hirokura, K. Iwasaki, T. Ido, R. Kumazawa, H. Kuramoto, T. Minami, I.. Nomura, M. Sasao, K.N. Sato, T. Tsuzuki, I. Yamada and T. Watari,
Potential Turbulence in Tokamak Plasmas; Oct. 1998
(IAEA-CN-69/EXP2/14)

NIFS-576 S. Murakami, U. Gasparino, H. Idei, S. Kubo, H. Maassberg, N. Marushchenko, N. Nakajima, M. Romé and M. Okamoto,

5D Simulation Study of Suprathermal Electron Transport in Non-Axisymmetric Plasmas, Oct. 1998 (IAEA-CN-69/THP1/01)

NIFS-577 S. Fujiwara and T. Sato,
Molecular Dynamics Simulation of Structure Formation of Short Chain Molecules, Nov. 1998

NIFS-578 T. Yamagishi,
Eigenfunctions for Vlasov Equation in Multi-species Plasmas Nov. 1998

NIFS-579 M. Tanaka, A. Yu. Grosberg and T. Tanaka,
Molecular Dynamics of Strongly-Coupled Multichain Coulomb Polymers in Pure and Salt Aqueous Solutions; Nov. 1998

NIFS-580 J. Chen, N. Nakajima and M. Okamoto,
Global Mode Analysis of Ideal MHD Modes in a Heliotron/Torsatron System: I. Mercier-unstable Equilibria; Dec. 1998

NIFS-581 M. Tanaka, A. Yu. Grosberg and T. Tanaka,
Comparison of Multichain Coulomb Polymers in Isolated and Periodic Systems: Molecular Dynamics Study; Jan. 1999

NIFS-582 V.S. Chan and S. Murakami,
Self-Consistent Electric Field Effect on Electron Transport of ECH Plasmas, Feb. 1999

NIFS-583 M. Yokoyama, N. Nakajima, M. Okamoto, Y. Nakamura and M. Wakatani,
Roles of Bumpy Field on Collisionless Particle Confinement in Helical-Axis Heliotrons, Feb. 1999

NIFS-584 T.-H. Watanabe, T. Hayashi, T. Sato, M. Yamada and H. Ji,
Modeling of Magnetic Island Formation in Magnetic Reconnection Experiment, Feb. 1999

NIFS-585 R. Kumazawa, T. Mutoh, T. Seki, F. Shinpo, G. Nomura, T. Ido, T. Watari, Jean-Marie Noterdaeme and Yangping Zhao,
Liquid Stub Tuner for Ion Cyclotron Heating, Mar. 1999

NIFS-586 A. Sagara, M. Iima, S. Inagaki, N. Inoue, H. Suzuki, K. Tsuzuki, S. Masuzaki, J. Miyazawa, S. Morita, Y. Nakamura, N. Noda, B. Peterson, S. Sakakibara, T. Shimozuma, H. Yamada, K. Akaishi, H. Chikaraishi, H. Funaba, O. Kaneko, K. Kawahata, A. Komori, N. Ohyabu, O. Motojima, LHD Exp. Group 1, LHD Exp. Group 2,
Wall Conditioning at the Starting Phase of LHD, Mar. 1999

NIFS-587 T. Nakamura and T. Yabe,
Cubic Interpolated Propagation Scheme for Solving the Hyper-Dimensional Vlasov-Poisson Equation in Phase Space, Mar. 1999

NIFS-588 W.X. Wnag, N. Nakajima, S. Murakami and M. Okamoto,
An Accurate δf Method for Neoclassical Transport Calculation, Mar. 1999

NIFS-589 K. Kishida, K. Araki, S. Kishiba and K. Suzuki,
Local or Nonlocal? Orthonormal Divergence-free Wavelet Analysis of Nonlinear Interactions in Turbulence, Mar. 1999

NIFS-590 K. Araki, K. Suzuki, K. Kishida and S. Kishiba,
Multiresolution Approximation of the Vector Fields on T^3; Mar. 1999

NIFS-591 K. Yamazaki, H. Yamada, K.Y.Watanabe, K. Nishimura, S. Yamaguchi, H. Nakanishi, A. Komori, H. Suzuki, T. Mito, H. Chikaraishi, K. Murai, O. Motojima and the LHD Group,
Overview of the Large Helical Device (LHD) Control System and Its First Operation; Apr. 1999

NIFS-592 T. Takahashi and Y. Nakao,
Thermonuclear Reactivity of D-T Fusion Plasma with Spin-Polarized Fuel; Apr. 1999

NIFS-593 H. Sugama,
Damping of Toroidal Ion Temperature Gradient Modes, Apr. 1999

NIFS-594 Xiaodong Li,
Analysis of Crowbar Action of High Voltage DC Power Supply in the LHD ICRF System; Apr. 1999

NIFS-595 K. Nishimura, R. Horiuchi and T. Sato,

Drift-kink Instability Induced by Beam Ions in Field-reversed Configurations; Apr. 1999

NIFS-596 Y. Suzuki, T-H. Watanabe, T. Sato and T. Hayashi,
Three-dimensional Simulation Study of Compact Toroid Plasmoid Injection into Magnetized Plasmas; Apr. 1999

NIFS-597 H. Sanuki, K. Itoh, M. Yokoyama, A. Fujisawa, K. Ida, S Toda, S.-I. Itoh, M. Yagi and A. Fukuyama,
Possibility of Internal Transport Barrier Formation and Electric Field Bifurcation in LHD Plasma; May 1999

NIFS-598 S. Nakazawa, N. Nakajima, M. Okamoto and N. Ohyabu,
One Dimensional Simulation on Stability of Detached Plasma in a Tokamak Divertor; June 1999

NIFS-599 S. Murakami, N. Nakajima, M Okamoto and J. Nhrenberg,
Effect of Energetic Ion Loss on ICRF Heating Efficiency and Energy Confinement Time in Heliotrons, June 1999

NIFS-600 R. Horiuchi and T. Sato,
Three-Dimensional Particle Simulation of Plasma Instabilities and Collisionless Reconnection in a Current Sheet;; June 1999

NIFS-601 W. Wang, M. Okamoto, N Nakajima and S. Murakami,
Collisional Transport in a Plasma with Steep Gradients; June 1999

NIFS-602 T Mutoh, R. Kumazawa, T Saki, K. Saito, F. Simpo, G. Nomura, T Watari, X Jikang, G. Cattanei, H. Okada, K. Ohkubo. M. Sato, S. Kubo, T. Shimozuma, H. Idei, Y. Yoshimura, O. Kaneko, Y. Takeiri, M Osakabe, Y. Oka, K. Tsumori, A. Komori, H. Yamada, K. Watanabe, S. Sakakibara, M. Shoji, R. Sakamoto, S. Inagaki, J Miyazawa, S Morita. K Tanaka, B J Peterson S Murakami T Minami, S. Ohdachi, S Kado, K. Narihara, H. Sasao, H Suzuki, K. Kawahata, N Ohyabu, Y. Nakamura, H Funaba, S. Masuzaki, S. Muto, K. Sato, T. Morisaki, S. Sudo, Y. Nagayama, T. Watanabe, M Sasao, K Ida, N. Noda, K Yamazaki, K Akaishi, A Sagara, K. Nishimura, T. Ozaki, K. Toi, O. Motojima, M Fujiwara, A. Iiyoshi and LHD Exp Group 1 and 2,
First ICRF Heating Experiment in the Large Helical Device , July 1999

NIFS-603 P.C. de Vries, Y. Nagayama, K. Kawahata, S. Inagaki, H. Sasao and K. Nagasaki,
Polarization of Electron Cyclotron Emission Spectra in LHD; July 1999

NIFS-604 W. Wang, N. Nakajima, M. Okamoto and S. Murakami,
δf Simulation of Ion Neoclassical Transport; July 1999

NIFS-605 T. Hayashi, N. Mizuguchi, T. Sato and the Complexity Simulation Group,
Numerical Simulation of Internal Reconnection Event in Spherical Tokamak; July 1999

NIFS-606 M. Okamoto, N. Nakajima and W. Wang,
On the Two Weighting Scheme for δf Collisional Transport Simulation: Aug. 1999

NIFS-607 O. Motojima, A.A. Shishkin, S. Inagaki, K. Y. Watanabe,
Possible Control Scenario of Radial Electric Field by Loss-Cone-Particle Injection into Helical Device; Aug. 1999

NIFS-608 R. Tanaka, T Nakamura and T Yabe,
Constructing Exactly Conservative Scheme in Non-conservative Form; Aug. 1999

NIFS-609 H. Sugama,
Gyrokinetic Field Theory; Aug. 1999

NIFS-610 M. Takechi, G. Matsunaga, S. Takagi, K.Ohkuni, K. Toi, M Osakabe, M. Isobe, S. Okamura, K. Matsuoka. A. Fujisawa, H. Iguchi, S. Lee, T Minami, K. Tanaka, Y. Yoshimura and CHS Group,
Core Localized Toroidal Alfven Eigenmodes Destabilized By Energetic Ions in the CHS Heliotron/Torsatron; Sep. 1999

NIFS-611 K. Ichiguchi,
MHD Equilibrium and Stability in Heliotron Plasmas; Sep. 1999

NIFS-612 Y. Sato, M. Yokoyama, M. Wakatani and V. D. Pusovitov,
Complete Suppression of Pfirsch-Schlüter Current in a Toroidal l=3 Stellarator; Oct. 1999